J Mater Sci: Mater Med (2010) 21:2947–2953
DOI 10.1007/s10856-010-4148-8

Low temperature fabrication of magnesium phosphate cement scaffolds by 3D powder printing

Uwe Klammert · Elke Vorndran · Tobias Reuther · Frank A. Müller · Katharina Zorn · Uwe Gbureck

Received: 16 May 2010 / Accepted: 6 August 2010 / Published online: 26 August 2010

Abstract Synthetic bone replacement materials are of great interest because they offer certain advantages compared with organic bone grafts. Biodegradability and preoperative manufacturing of patient specific implants are further desirable features in various clinical situations. Both can be realised by 3D powder printing. In this study, we introduce powder-printed magnesium ammonium phosphate (struvite) structures, accompanied by a neutral setting reaction by printing farringtonite ($Mg_3(PO_4)_2$) powder with ammonium phosphate solution as binder. Suitable powders were obtained after sintering at 1100°C for 5 h following 20–40 min dry grinding in a ball mill. Depending on the post-treatment of the samples, compressive strengths were found to be in the range 2–7 MPa. Cytocompatibility was demonstrated in vitro using the human osteoblastic cell line MG63.

Keywords 3D powder printing · Magnesium phosphate cement · Struvite · Bone replacement material

U. Klammert (✉) · T. Reuther
Department of Cranio-Maxillo-Facial Surgery, University of Würzburg, Pleicherwall 2, 97070 Würzburg, Germany
e-mail: klammert_u@klinik.uni-wuerzburg.de

E. Vorndran · U. Gbureck
Department for Functional Materials in Medicine and Dentistry, University of Würzburg, Pleicherwall 2, 97070 Würzburg, Germany

F. A. Müller · K. Zorn
Institute of Materials Science and Technology (IMT), Friedrich-Schiller-University of Jena, Löbdergraben 32, 07743 Jena, Germany

1 Introduction

The demand for synthetic bone replacement materials is still relentless due to their advantages of having a well-defined chemistry and architecture, unlimited availability without causing any donor site morbidity and the exclusion of transmission of infections compared with homologous or xenogenous grafts. Because of the chemical similarity to the mineral phase of bone, favoured synthetic materials are based on calcium phosphate chemistry. These materials are usually applied as solid structures of β-tricalcium phosphate (β-TCP) [1] or hydroxyapatite (HA) [2] as well as self-setting cements [3].

Calcium phosphate cement (CPC) formation is based on the different pH-dependent solubility of cement reactants and the final setting product, which is either hydroxyapatite (HA) at pH > 4.2 or dicalcium phosphate dihydrate (brushite) at pH < 4.2 [4]. Since self-setting cements may offer an inconvenient workability because they are difficult to mould in various clinical situations [5], prefabricated solid implants with a patient-tailored shape are desirable. Furthermore, biodegradability in physiological conditions accompanied by osteoconductive features could be preferable. The manufacturing of such implants with the aid of rapid prototyping (rp) can be considered as state of the art because the direct CAD/CAM processing using the patient's imaging data (e.g., computed tomography scans) may help to reduce error sources [6–8]. Depending from the rp technique, a high fitting precision can be realised [9, 10]. A very attractive rp technique is the 3D powder printing, since it is performed at room temperature and thus the processing of thermo-sensitive additives, e.g., bioactive substances, is basically possible. Furthermore, the technique enables the spatial distribution of such additives.

The 3D powder printing of dicalcium phosphate dihydrate (brushite) structures has been reported previously [11–13]. The brushite material offers numerous suitable features concerning biocompatibility, biodegradability and mechanical performance for non- or low load-bearing defects. The direct modification with certain additives was reported as well [14, 15]. However, the transient acidic environment during the printing process, which is caused by the liquid phase phosphoric acid, could be disadvantageous as far as acid-labile additives are supposed to be processed.

Therefore the current study aimed to investigate the fabrication of 3D powder-printed magnesium ammonium phosphate (struvite, $MgNH_4PO_4\ 6H_2O$) structures. Cement formulations, which forms struvite as the setting product, were described several times in the literature [16–19]. Here, we introduce the magnesium ammonium phosphate chemistry into 3D powder printing. The printing process was performed at neutral pH since farringtonite powder was combined with diammonium hydrogen phosphate/ammonium dihydrogen phosphate as liquid printing phase, leading to the formation of struvite. The setting products were characterised by their phase composition and mechanical performance and the in vitro cytocompatibility was evaluated using the osteoblastic cell line MG63. For estimation of the chemical behaviour in a wet environment, free electrolytes and pH value of the supernatant cell culture medium were analysed.

2 Materials and methods

2.1 Powder preparation and printing process

Farringtonite powder ($Mg_3(PO_4)_2$) was prepared by mixing magnesium hydroxide ($Mg(OH)_2$, Fluka, Seelze, Germany) and magnesium hydrogen phosphate trihydrate ($MgHPO_4{\cdot}3H_2O$, Sigma-Aldrich, Steinheim, Germany) in appropriate stoichometry and sintering at 1100°C for 5 h. The sintered farringtonite cake was crushed with mortar and pestle, ground at 200 min^{-1} for 10–60 min in a planetary ball mill (PM400, Retsch, Haan, Germany) and sieved with a 355 µm pore size mesh. Finally, the ground powder was blended with 20% diammonium hydrogen phosphate sieved < 355 µm ($(NH_4)_2HPO_4$, DAHP, Merck, Darmstadt, Germany) in a mixer (M5R, Lödige, Paderborn, Germany). The binder solution was prepared by mixing 0.75 M $(NH_4)_2HPO_4$ and 0.75 M $NH_4H_2PO_4$ (Merck, Darmstadt, Germany).

The structures were printed at room temperature using a commercial 3D-powder printing system (Z-Corporation, Burlington, USA) using the following parameters: 125 µm layer thickness and a binder powder volume ratio of 0.371. The solidification of the printing objects occurred according to Equation 1:

$$2Mg_3(PO_4)_2 + 3(NH_4)_2HPO_4 + 36H_2O \rightarrow 6MgNH_4PO_4{\cdot}\ 6H_2O + H_3PO_4 \quad (1)$$

The scaffolds were computer-aided designed using STL (stereolithography) data, having a cylindrical shape with a diameter of 15 mm and a height of 2 mm for cell culture. After the printed samples were dried in ambient conditions for 24 h, subsequently, the specimens were post-hardened by immersion in the binder solution for 24 h. Finally, the scaffolds were rinsed three times with distilled water, soaked with 70% ethanol and air-dried.

2.2 Phase composition, particles size, setting time and mechanical properties

X-ray diffraction patterns were recorded on a D 5005 diffractometer (Siemens, Karlsruhe, Germany). Data were collected from $2\theta = 20$ to 40° with a step size of 0.02° using Cu-K_α radiation. Particle sizes of farringtonite powder of different grinding times (10, 20, 40 and 60 min) were measured with a particle size distribution analyzer LA-300 (Horiba, Kyoto, Japan) by dispersing approximately 100 mg powder in isopropyl alcohol. For the setting time, 2 g of powder and 600 µl binder (powder/liquid ratio = 3) were mixed with a spatula on a glass plate and formed to a cube. The setting process is considered to be complete if the sample is hard and no longer plastic.

Compressive strength testing was performed at a crosshead speed of 1 mm/min using a static mechanical testing device Zwick 1440 (Zwick, Ulm, Germany) with a 5kN load cell. For this purpose, pure and DAHP-modified farringtonite cylindrical samples with an aspect ratio of 2:1 (d = 5 mm, h = 10 mm) were prepared as described above and aged in double-distilled water or in binder solution for 24 h prior to testing.

2.3 Cell culture

Human osteoblastic cells (osteosarcoma-derived cell line MG63, ATCC No. CRL-1427, Rockville, MD, USA) were cultured in Dulbecco's modified Eagle's Medium (DMEM, Invitrogen, Karlsruhe, Germany) supplemented with 10% fetal calf serum and 1% penicillin and streptomycin, respectively, all from Invitrogen, in a humidified 5% CO_2 atmosphere at 37°C. The struvite cell culture scaffolds (15 mm diameter, 2 mm height) as well as standard positive (cp-titanium) and negative (copper) control specimens with the same geometric dimension were placed into the cavities of 24 well plates (Greiner, Frickenhausen, Germany). The control specimens were used as received, as

cold rolled metal sheet. Without further surface-treatment they were sonicated and cleaned with detergent and autoclaved at 134°C for 2 h. As further controls served cell culture dishes (Polystyrene, PS) without any specimens. The cells were seeded as a suspension with 2 ml medium per well in a concentration of 5×10^4/well onto the prepared specimens. Cells were cultured for 10 days and the medium was changed every second day. The assays were performed on day 2, 4, 6, 8 and 10 within three independent experiments with n = 12 (test specimens) and n = 4 (controls) each time, respectively.

2.3.1 Cell viability

For evaluation of the cell viability, the WST-1 Kit (Roche Diagnostics, Mannheim, Germany) was used. After incubating the cells for 15 min with the WST reagent 1:10 in fresh DMEM at 37°C, 100 µl of the supernatant was transferred into 96 well microtiter plates. The absorption of the supernatant was quantified photometrically at 440 nm (Tecan Rainbow, Tecan, Crailsheim, Germany).

2.3.2 Chemical analysis of the culture medium

For assessment of the chemical behaviour of the scaffolds under cell culture conditions, the supernatant culture medium was collected within the medium changes every second day. The concentrations of free calcium, magnesium and phosphate ions as well as pH-values were investigated. The measurement of the electrolyte concentration was performed by the use of commercial complex forming test systems, which are also applied in the clinical routine (Cobas Integra in vitro diagnostics laboratory system, Roche Diagnostics, Mannheim, Germany). The pH-values were measured with a pH meter (inoLab pH Level 1 combined with a SenTix 61 electrode, WTH, Weilheim, Germany).

2.3.3 Scanning electron microscopy

For visualisation of cell growth and cell morphology, the cell bearing scaffolds underwent scanning electron microscopy (SEM) (FEI, Quanta 200, Czech Republic). Therefore, the specimens were rinsed in PBS and underwent a fixation procedure with ice-cold glutaraldehyde (6% in PBS, Merck, Darmstadt, Germany). After 4 rinses in PBS, cells were dehydrated in ascending concentrations of acetone (30, 50, 75, 90 and 5 times in 100%, Sigma-Aldrich, Taufkirchen, Germany). After critical point drying (CPD 030 BAL-TEC, Balzers, Liechtenstein), the samples were coated with gold (K550, EMITECH, Kent, UK) and analyzed by SEM.

2.4 Statistics

Data of the in vitro investigations were normally distributed. Variance analysis and statistical calculations were performed with the program SPSS 17, SPSS Inc., Chicago, USA. For comparision of struvite against each of the controls, a *t*-test for independent samples was chosen and significance levels were set at $p < 0.05$.

3 Results and discussion

3.1 Cement preparation and 3D printing of the scaffolds

Ahead of this study the farringtonite powder was optimised for 3DP processability concerning setting time, bulk density and spreadability. For introduction in 3DP, powders must fulfil two crucial criteria. Firstly they must permit the formation of thin and smooth layers of 100–200 µm thickness, and secondly they must rapidly harden with the binder solution during printing. The first criterion is influenced by the particle size distribution of the powder. It was previously demonstrated that ideal particle sizes are in the range of 20–50 µm excluding small particle fractions < 5 µm [6]. Otherwise the formation of large and stable agglomerates (up to 1–2 mm in diameter) would occur, preventing an accurate printing result. A further possibility to obtain an optimal spreadability of the powder is given by using a broad particles size distribution with only a small fine particle fraction. As it is shown in Figure 1 for 10–40 min ground powders, a plane powder surface (not displayed) correlated with a bimodal particle size distribution containing a broad fraction of big size particles in the range of 10–100 µm with a minor fraction of particles smaller than 10 µm and a d_{50} value of about 27 µm. After 60-min grinding, the fine fraction (<10 µm) rises, which involved a decreasing d_{50} value to 19 µm and results in an agglomeration of powder particles. The groove-like surface of 60 min ground powder is incompatible with the printing process due to a loss of printing accuracy. The second criterion depends on the reactivity of the cement, including the velocity of the cement-setting reaction and the strength of the setting product. If the reaction is too slow, the binder liquid spreads through the powder driven by capillary forces, also leading to inaccurate printing results. Furthermore the samples have to be strong enough to guarantee a non-destructive removing and dedusting from the surrounding powder. Both could be achieved by modification of the most reactive pure farringtonite powder (20 min ground, Table 1) with 20% of DAHP. By this, the setting time as well as the cement conversion rate (Fig. 2) to struvite correlated with the increased mechanical performance

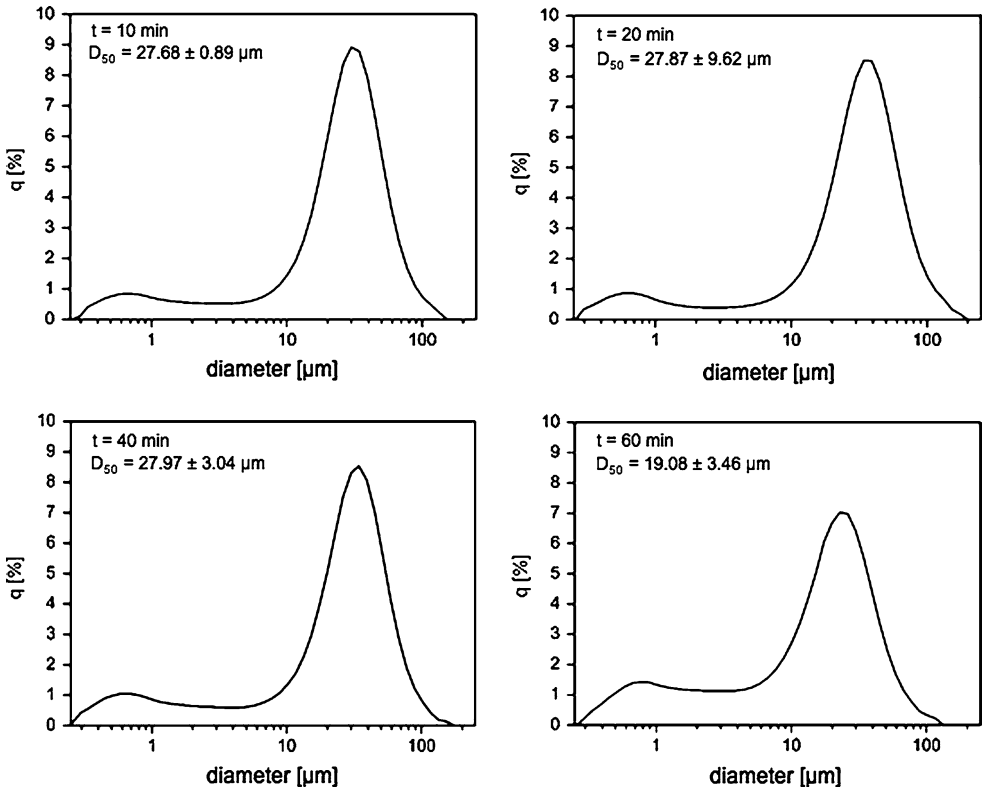

Fig. 1 Particle size distribution after different grinding times (10–60 min). The particle size is shifting to a broad bimodal distribution with increasing grinding time

Table 1 Cement setting time of pure and DAHP-modified farringtonite powder (20 min ground) and a powder/liquid-ratio of 3

Powder	Setting time/min
$Mg_3(PO_4)_2$	2.5
$Mg_3(PO_4)_2$ modified with 20% DAHP	26

(Table 2). Consequently, the processability and dimensional precision of the structures could be improved by DAHP modification compared with pure farringtonite powder.

3.2 Phase composition and mechanical properties

Typical X-ray diffraction patterns of the 3D printed magnesium ammonium phosphate cement are shown in Fig. 2. The raw starting powder was identified to be phase pure farringtonite ($Mg_3(PO_4)_2$, PDF-No. 33-0876). The degree of cement conversion immediately after printing was relatively low as indicated by the only weak struvite (PDF-No. 15-0762) signal at $2\theta = 20.9°$ and weak compressive strengths of the specimens. For improvement of the cement conversion rate (Fig. 2) and thus for mechanical reinforcement (Table 2), farringtonite powder was (1) modified with 20% DAHP powder and (2) the printed structures were post-hardened by immersion in the binder solution for 24 h. Both process modifications strongly increased the degree of conversion to struvite as it can be seen by an increase of reflection peak intensity of struvite and a decrease of the farringtonite peak intensity in XRD. As a by-product a small amount newberryite ($MgHPO_4 \cdot 3H_2O$, PDF-No. 35-0780) was formed.

3.3 Cell culture

3.3.1 Cell viability

Over the course of 10 days, the cell viability within the struvite cultures increased continually until day 8, followed by a slight decline on day 10. Positive control cultures, both titanium and PS, respectively, also presented a continual increase from day 2 till day 8, with a markedly decrease on day 10. Compared to the positive controls, the cell viability of the struvite cultures was significantly inferior, up to nearly 60% (day 10, compared with PS). As expected, the negative control cultures showed no cell growth in an effective manner, due to the cytotoxicity of copper (Fig. 3). The data indicates a reduced cytocompatibility of the powder printed struvite scaffolds in vitro. This behaviour could be caused by chemical features of the ceramic surface, e.g., partial dissolution in physiological environment, resulting in changes of the ion concentrations of the cell culture medium (see below). Decrease of cell viability on day 10, which was observed in the struvite and

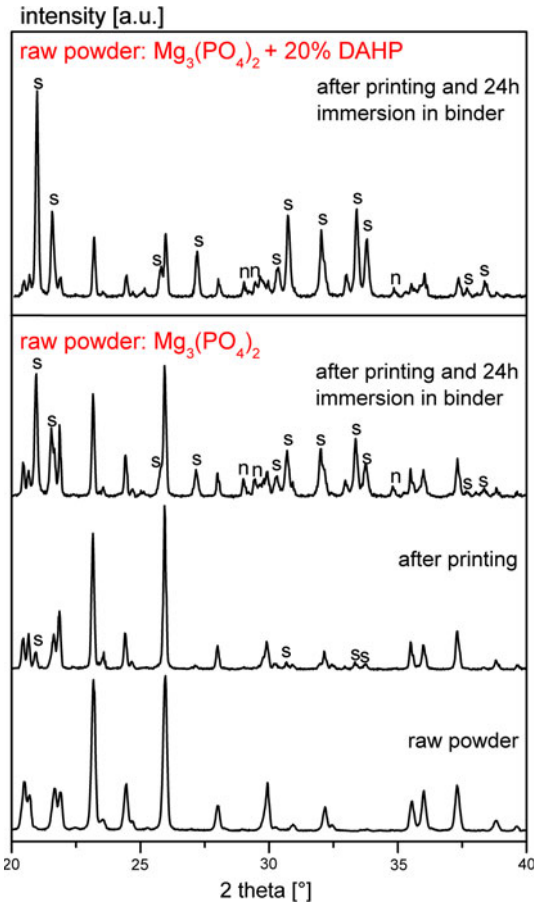

Fig. 2 XRD of magnesium phosphate raw powder (farringtonite), powder after printing, and powder after printing and immersion in 0.75 M AHP + 0.75 M DAHP-binder solution for 24 h. Most relevant peaks are marked for struvite(s) and newberryite (n). Unlabeled peaks correspond to farringtonite

Table 2 Compressive strength of printed and post-treated struvite samples (n = 10)

Post-treatment conditions	Compressive strength/MPa	
	$Mg_3(PO_4)_2$	$Mg_3(PO_4)_2$ modified with 20% DAHP
After printing	0.23 ± 1.37	2.12 ± 0.40
After printing and immersion in H_2O	0.82 ± 0.15	2.92 ± 0.39
After printing and immersion in binder	7.01 ± 1.37	6.26 ± 1.73

in the positive control cultures as well, certainly results from reaching a dense cell culture stage.

3.3.2 *Chemical analysis of the culture medium*

The pH-values of the struvite cell culture medium have never been beyond a physiological range and rated in the same magnitude compared with the medium of the titanium and PS control cultures. The differences were partly significant, partly they were not (Fig. 4a). In all groups except copper the pH-values were somewhat lower than that of fresh culture medium (pH 8.03) due to cell metabolism. The concentrations of free Mg^{2+} ions were significantly enhanced within the struvite cell culture medium. Whereas the values of the controls remained constant over the course, the Mg^{2+} concentration of the struvite cultures was nearly 8.6-fold increased at the beginning (day 2) and declined continually and significantly over the course of 10 days until it was nearly 7.1-fold increased at day 10 (Fig. 4b). The same behaviour was observed regarding free PO_4^{3-} ions (Fig. 4c). The concentrations of the struvite cultures were significantly increased, nearly 7.5-fold at day 2, and continually and significantly declined until day 10 (nearly 5.2-fold).

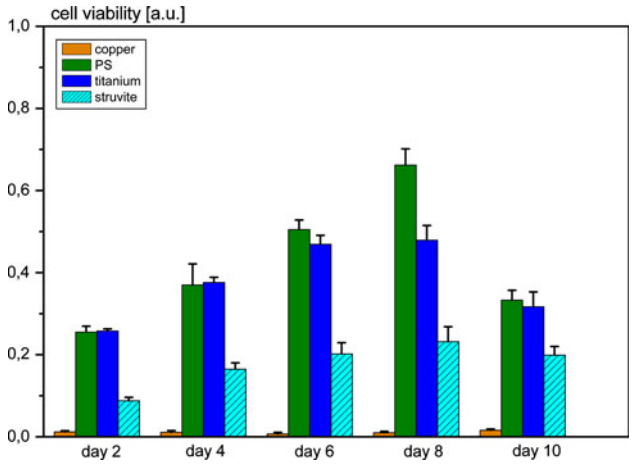

Fig. 3 Cell viability of MG63 cultured on 3D powder printed magnesium ammonium phosphate (struvite) scaffolds compared with positive (titanium and PS) and negative (copper) controls. The differences between struvite and each of the controls are always significant ($p < 0.05$). Results are displayed as mean of n = 12 specimens ± standard deviation

A converse situation was noticed concerning the concentration of free Ca^{2+} ions. In the struvite cell culture medium, it was significantly reduced compared with the controls (nearly 50% at day 2) and showed a slight but significant increase up to nearly 60% at the end of the course (Fig. 4d). The observed electrolyte alterations of the struvite cell culture medium do result from the considerable solubility of the powder printed struvite ceramic. Because the supernatant medium was refreshed every second day, the concentrations of free Mg^{2+} and PO_4^{3-} ions decreased gently over the course of 10 days. Since calcium phosphates have lower solubility than magnesium phosphates, calcium ions originally of the culture medium are precipitated by the abundant phosphate ions, leading to a decrease of free Ca^{2+} ions. However, these alterations of

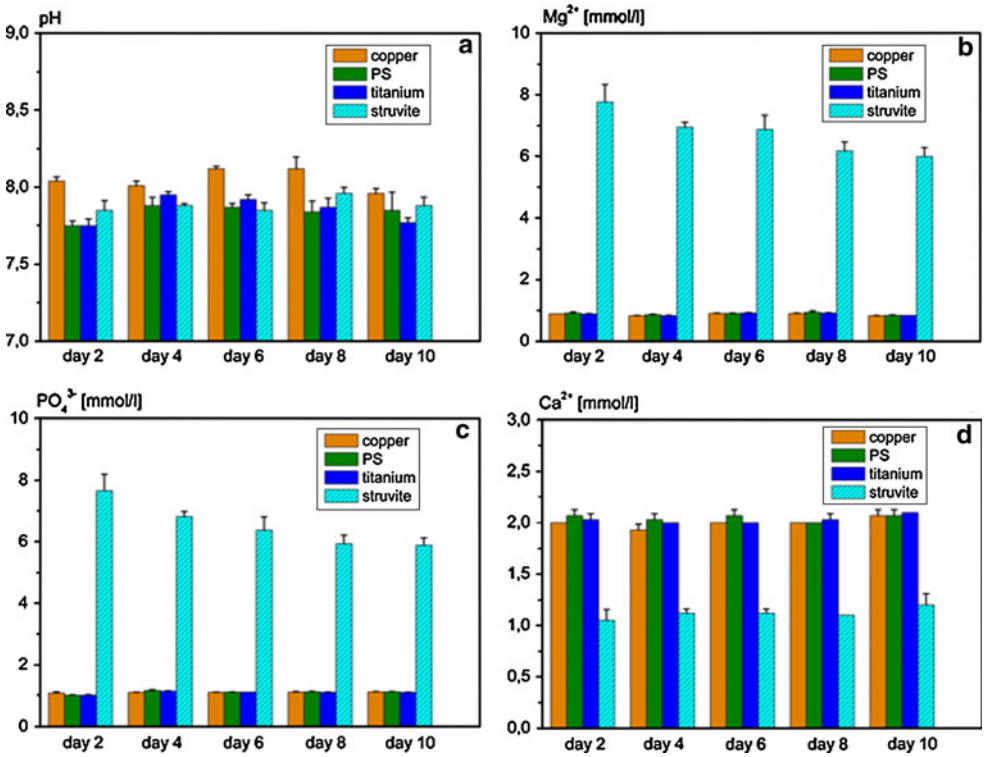

Fig. 4 Assessment of pH-values of the cell culture medium (**a**). Merely slight and irregular increasing compared to the titanium and PS control cultures, partly significant (day 2, 8, and 10 only compared to titanium). The concentrations of free Mg^{2+} (**b**) and PO_4^{3-} (**c**) ions of the struvite cultures are significantly higher, and the concentrations of free Ca^{2+} ions are significantly lower than that of the controls (**d**). Results are displayed as mean of n = 6 specimens ± standard deviation

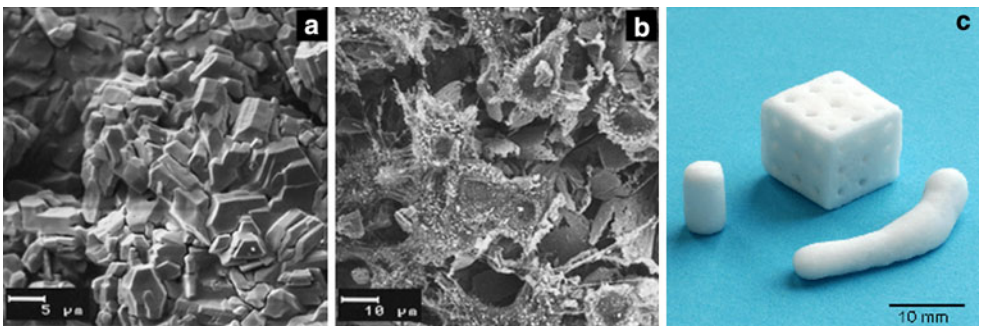

Fig. 5 Scanning electron microscopy (SEM) of the magnesium ammonium phosphate (struvite) matrices immediately after fabrication (**a**) and after seeding of MG63 cells at the middle of the course of 10 days (**b**). Additionally, some macrostructures (cylinder, cuboid, part of orbital rim) are shown in (**c**)

free electrolytes with possible adverse effects to cytocompatibility in vitro should be negligible in vivo at a sufficiently vascularised implantation site leading to a continuous fluid exchange compared with the cell culture model with discontinuous fluid refreshment merely every second day.

3.3.3 Scanning electron microscopy

SEM of the surface of the powder printed struvite matrices showed crystals with different sizes and blunt edges (Fig. 5a). A typical micrograph of a cell bearing struvite scaffold at the end of the course of 10 days is shown in Fig. 5b. The rough surface of the material with the abundant osteoblastic cells is clearly to be seen.

4 Conclusion

The current study demonstrated for the first time 3D powder printing of magnesium ammonium phosphate (struvite) cell culture scaffolds. The magnesium phosphate powder was produced by sintering mixtures of $Mg(OH)_2$ and $MgHPO_4{\cdot}3H_2O$ at temperature of 1100°C and optimised for 3DP concerning setting time, bulk density, spreadability and the mechanical performance of the

printed matrix. Cell culture studies indicated a suitable cytocompatibility for osteoblastic cells. The reduced cell viability compared with the titanium and polystyrene controls is likely resulting from the considerable solubility of the struvite structures in a wet environment as indicated by significantly altered free electrolytes of the cell culture medium. Due to the current results we conclude that the magnesium ammonium phosphate cement introduced here provides suitable features for its use as material for hard tissue regeneration. The processability at room temperature using the 3D printing technique as well as the setting reaction at neutral pH would enable the direct modification with thermo- and acid-labile additives. Further in vivo investigations are required to prove other biological features like resorption kinetics at the implantation site and osteo-conductive properties.

Acknowledgments The authors would like to acknowledge the financial support from the Deutsche Forschungsgemeinschaft (DFG Gb1/11-1, DFG Mu1803/7-1 and DFG Kl2400/1-2).

References

1. Geros RZ. Properties of osteoconductive biomaterials: calcium phosphates. Clin Orthop. 2002;39:81–98.
2. Rosen HM, Ackermann JL. Porous block hydroxyapatite in orthognatic surgery. Angle Orthod. 1991;61:185–91.
3. Bohner M, Gbureck U, Barralet JE. Technological issues for the development of more efficient calcium phosphate bone cements: a critical assessment. Biomaterials. 2005;26:6423–9.
4. Dorozhkin SV. Calcium orthophosphate cements for biomedical applications. J Mater Sci. 2008;43:3028–57.
5. Hollier LH, Stal S. The use of hydroxyapatite cements in craniofacial surgery. Clin Plast Surg. 2004;31:423–8.
6. Webb PA. A review of rapid prototyping (RP) techniques in the medical and biomedical sector. J Med Eng Technol. 2000; 24:149–53.
7. Ashley S. Rapid prototyping for artificial body parts. Mech Eng (USA). 1993;115:50–3.
8. Peters F, Groisman D, Davids R, Hanel T, Durr H, Klein M. Comparative study of patient individual implants from beta-tricalcium phosphate made by different techniques based on CT data. Materialwissensch Werkstofftech. 2006;37:457.
9. Ibrahim D, Broilo TL, Heitz C, de Oliveira MG, de Oliveira HW, Nobre SM, Dos Santos Filho JH, Silva DN. Dimensional error of selective laser sintering, three-dimensional printing and PolyJet models in the reproduction of mandibular anatomy. J Craniomaxillofac Surg. 2009;37:167–73.
10. Silva DN, de Oliveira MG, Meurer E, Meurer MI, Lopes da Silva JV, Santa-Barbara A. Dimensional error in selective laser sintering and 3D-printing of models for craniomaxillary anatomy reconstruction. J Craniomaxillofac Surg. 2008;36:443–9.
11. Gbureck U, Hölzel T, Klammert U, Würzler K, Müller FA, Barralet JE. Resorbable dicalcium phosphate bone substitutes prepared by 3D powder printing. Adv Funct Mater. 2007;17:3940–5.
12. Vorndran E, Klarner M, Klammert U, Grover LM, Patel S, Barralet JE, Gbureck U. 3D powder printing of β-Tricalcium phosphate ceramics using different strategies. Adv Eng Mater. 2008;10:B67–71.
13. Klammert U, Reuther T, Jahn C, Kraski B, Kübler AC, Gbureck U. Cytocompatibility of brushite and monetite cell culture scaffolds made by three-dimensional powder printing. Acta Biomater. 2009;5:727–34.
14. Gbureck U, Vorndran E, Müller FA, Barralet JE. Low temperature direct 3D printed bioceramics and biocomposites as drug release matrices. J Control Release. 2007;122:173–80.
15. Vorndran E, Klammert U, Ewald A, Barralet JE, Gbureck U. Simultaneous immobilization of bioactives during 3D powder printing of bioceramic drug-release matrices. Adv Funct Mater. 2010;20:1585–91.
16. Driessens FCM, Boltong MG, Wenz R, Meyer J. Calcium phosphates as fillers in struvite cements. Key Eng Mater. 2005;284–286:161–4.
17. Hall DA, Stevens R, El Jazairi B. Effect of water content on the structure and mechanical properties of magnesia-phosphate cement mortar. J Am Ceram Soc. 1998;81:1550–6.
18. Hipedinger NE, Scian AN, Aglietti EF. Magnesia-ammonium phosphate-bonded cordierite refractory castables: phase evolution on heating and mechanical properties. Cem Concr Res. 2004;34:157–64.
19. Sarkar AK. Hydration/dehydration characteristics of struvite and dittmarite pertaining to magnesium ammonium phosphate cement systems. J Mater Sci. 1991;26:2514–8.